Patterns of blood flow during the postprandial response in ball pythons, *Python regius*

J. Matthias Starck* and Christian Wimmer

Department of Biology II, University of Munich (LMU), Großhaderner Strasse 2, D-82152 Planegg-Martinsried, Germany

*Author for correspondence (e-mail: starck@uni-muenchen.de)

Summary

We present evidence supporting the hypothesis that postprandial upregulation of the size of the small intestine and the liver is caused by an increased blood flow volume to the organs. The postprandial response of ball pythons was characterized by measurements of oxygen consumption, organ size changes and histological evaluation of the mucosal epithelium and liver parenchyme. Synchronized with these changes in measurements were changes in the patterns of blood flow volume to small intestine and liver. A correlation analysis of organ size change and blood flow volume showed a significant nonlinear relationship, which explained about 50% of the overall variances in organ size (small intestine, liver). Histological analysis indicated that incorporation of lipid droplets in enterocytes and in hepatocytes contributes to an increase of absorptive surface magnification (in small intestine) and hepatocyte size (in liver). Collectively, these data support the concept that in the ball python, postprandial upregulation of organ size does not reflect new mitotic activity, but rather results from increased blood volume in the intestinal villi and incorporation of lipid droplets into enterocytes and hepatocytes, respectively.

Key words: postprandial response, ball python, *Python regius*, Doppler-ultrasonography, organ size change.

Introduction

The postprandial response of snakes and many other reptiles is characterized by a metabolic upregulation (specific dynamic action, SDA), together with an increase in organ sizes, in particular of the gastrointestinal tract and the liver. The upregulation of the gastrointestinal system is fast and a threefold increase of total organ size can be observed within 24–48 h after feeding. *Python* species have been intensively studied over recent years as an ectotherm model system and there has been significant progress in understanding the energy allocation during SDA and the structural and functional upregulation of the gastrointestinal system (Secor et al., 1994; Secor and Diamond, 1995, 1997, 1998, 2000; Overgaard et al., 1999, 2002; Thompson and Withers, 1999; Bedford and Christian, 2001; Starck and Beese, 2001, 2002; Secor, 2003; Starck et al., 2004; Wang et al., 2003, 2005; Andrade et al., 2005; Starck, 1999, 2003, 2005; McCue et al., in press). The threefold increase in size of the small intestine is associated with a configuration change of the mucosal epithelium, which changes from a pseudostratified epithelium into a single layered, high prismatic epithelium within 24–48 h after feeding (Starck and Beese, 2001, 2002; Starck, 2003, 2005). The upregulation of organ size is energetically cheap (Overgaard et al., 2002), i.e. only 5% of energy involved in overall SDA is used for the size increase of the small intestine (Secor, 2003). Supported by histological and anatomical data, Starck and Beese (2001, 2002) suggested that small intestinal size increases might be driven by a hydraulic system, i.e. blood and lymphatic fluid is pumped into the vessels of the connective tissue core of the villi, which consequently inflate (i.e. elongate) and provide an increased absorptive surface.

The hydraulic hypothesis predicts that the size increase of the small intestine and the liver is correlated with increasing blood flow volume into these organs within 24 h after feeding. Testing for such a relationship has only recently become possible by using noninvasive ultrasonographic imaging, which allows repeated and synchronized measurements of organ size and blood flow volume in unrestrained snakes (Starck and Burann, 1998; Starck et al., 2001). In the present work, we measured changes of blood flow volume in the major vessels supplying the small intestine and the liver in response to feeding and fasting during several postprandial periods. Synchronized with those measurements of blood flow volume we measured organ size changes and oxygen consumption to characterize SDA. To study changes of tissue configuration and cell morphometry, tissue samples were taken from a second group of snakes exposed to the same conditions.

Materials and methods

Animals and animal husbandry

All physiological measurements were made on six juvenile captive-raised pythons *Python regius* Shaw 1802 (body mass range 280–420 g; CITES no.: E0343/02) maintained in the reptile room at Department of Biology, University of Munich. Histological measurements were made on eight juvenile animals maintained under similar conditions in the Department of Zoophysiology, University of Aarhus. Animals were housed in 50 cm × 50 cm × 80 cm cages, with water, heating and shelter. Cage temperature ranged from 25–30°C, air humidity was 70%, and photoperiod was 12 h:12 h L:D. Snakes were fed live mice at intervals of approximately 4 weeks, i.e. on days 02, 30, 65 and 93 after the beginning of the experiment. Meal size was approximately 25% of the snake's body mass. The net gain in body mass of snakes was on average 7% after one meal. The snakes had been kept in the laboratory for approximately 1 year prior to experimentation and had been used in previous non-invasive studies (Starck et al., 2004). All physiological measurements were taken repeatedly from six individual snakes over a period of 4 months, i.e. four feeding cycles. The histological samples originate from eight juvenile snakes at the Department of Zoophysiology at Aarhus University, Denmark. Of those, four snakes had been fasted for 4 weeks, two snakes had been fed 48 h and the other two snakes for 24 h, before they were killed.

Doppler-Ultrasonography

A Technos MP (Esaote Biomedica, Genua, Italy) was used for ultrasound imaging and Doppler-ultrasonography. The Technos MP was equipped with a broad-band linear array scanner head (LA424, 8–14 MHz), which was used for all ultrasonography functions in this study, i.e. imaging, continuous wave Doppler (CW, for detection of blood flow in vessels) and pulsed wave Doppler (PW, for measurement of blood flow velocity). The LA424 scanner head is designed for high-resolution ultrasonography at close range (skin diagnosis and surface vessels) and has a spatial resolution of 0.4 mm laterally and 0.15 mm axially. The scanner head was operated with a penetration depth of 21 mm and the focus level adjusted flexibly. When using the PW-Doppler, a pulse repetition frequency of 4.0 kHz was used, allowing for the detection of low flow velocities. The PW-Doppler function provides a spectrum of velocities, which can be integrated over time to render time-averaged velocity (*TAV*, in m s^{-1}). If the cross-sectional area of the vessel is known, blood flow volume can be calculated as *TAV*×cross section of vessel×60 (ml min^{-1}). PW-Doppler measurements were taken from: (1) the A. mesenterica, (2) the liver portal vein *(Vena portae hepaticae)* and (3) the liver vein (Vena hepatica*)*. See below for anatomical and physiological implications of the measurement positions.

Dissections

Two preserved *Python regius* specimens (snout–vent length, *SVL*, 105 cm and 90 cm) were obtained from the Zoologische Staatssammlung, Munich, for macroscopic dissections of the vascular system. The two specimens were of unknown origin and had no inventory number; however, they were in perfect anatomical condition and had neither external nor internal injuries, nor pathologies.

Respirometry

Oxygen consumption was measured using an open flow system (FOX Field Oxygen Analyzer, Sable Systems, Las Vegas, NV, USA). Oxygen consumption of six snakes (mean body mass=147±34 g) was measured once per day starting 3 days before feeding and continued until 11 days after feeding. Thereafter, measurements were made every third day until 2 days before the next feeding, when daily measurements resumed. Measurements were taken at 30°C in the dark for 90–120 min; to minimize circadian effects each individual snake was measured at the same time of day, i.e. between 10:00 and 13:00 h. The volume of the metabolic chamber was 1200 ml. The air stream (35 ml min^{-1}) was dried (using silica gel blue, Roth GmbH, Germany) before entering the metabolic chamber. The air stream vented from the metabolic chamber to the O_2-analyzer was redried before entering the oxygen analyzer. We calculated mass-specific rate of oxygen consumption $\dot{V}_{O_2}$ (ml g^{-1} h^{-1}), corrected for standard temperature and pressure, by taking the lowest 10 min interval that did not change for more than 0.01% O_2-concentration. Metabolic data were analyzed using Data Can software (Sable Systems Inc.). Each day, rate of oxygen consumption was measured at the same time to avoid circadian pattern in metabolic rate affecting the results. A respiratory quotient of 0.8 was assumed for the strictly carnivorous animals.

Histology

The eight snakes from the Aarhus laboratory were killed by an overdose of pentabarbiturate (Nembutal). Immediately thereafter, they were dissected macroscopically and the small intestine and the liver preserved in 5% paraformaldehyde in 0.1 mol l^{-1} phosphate buffer at pH 7.4 and 4°C for at least 48 h. For histology, tissue samples of the small intestine and liver were washed in buffer, dehydrated through a graded series of ethanol to 96% ethanol and embedded in hydroxyethyl methacrylate (Historesin Leica Microsystems, Nußloch, Germany). Embedded material was sectioned into short series of 50 sections per sample (section thickness was 2 μm), mounted on slides, and stained with Methylene-Blue Thionine. Histological sections were studied using an Axioplan research microscope (Zeiss) equipped with a digital camera (Nikon Coolpix 990) and connected to the image-analysis and morphometry system. SigmaScanPro (v. 4.0, Jandel Scientific, SPSS Inc., Chicago, IL, USA) was used for imaging and morphometry.

Ultrasound morphometry and statistics

Ultrasound morphology and landmarks for morphometry of thickness of mucosa and cross-section of the liver have been described in previous studies (Starck and Beese, 2001, 2002; Starck et al., 2001, 2004; Starck, 2005). Briefly, a minimum of

Fig. 1. Vascular anatomy of ball python. (A–C) Right is cranial, left is caudal, top is ventral, and bottom is dorsal; (D,E) cross-sectional ultrasonographs, ventral is top of images. (A) Schematic drawing of major arteries (adopted from Hafferl, 1933). (B) Situs dissection of the aorta with branches of the mesenteric arteries. The gall bladder had been removed, the broken line indicating its original position. (C) Doppler-ultrasonographic anatomy of the aorta and first mesenteric artery. Color coding indicates direction and velocity of the blood stream. (D) Doppler-ultrasonographic anatomy of the liver (cross-section) and pulse waved (PW)-Doppler measurements from the liver portal vein (blue). Two small lung-arteries (red) run outside the liver. (E) PW-Doppler from the liver vein (blue). Liver vein and portal vein are opposite each other, blood flow is in the same direction. Portal vein and liver vein are interconnected by numerous sinusoids.
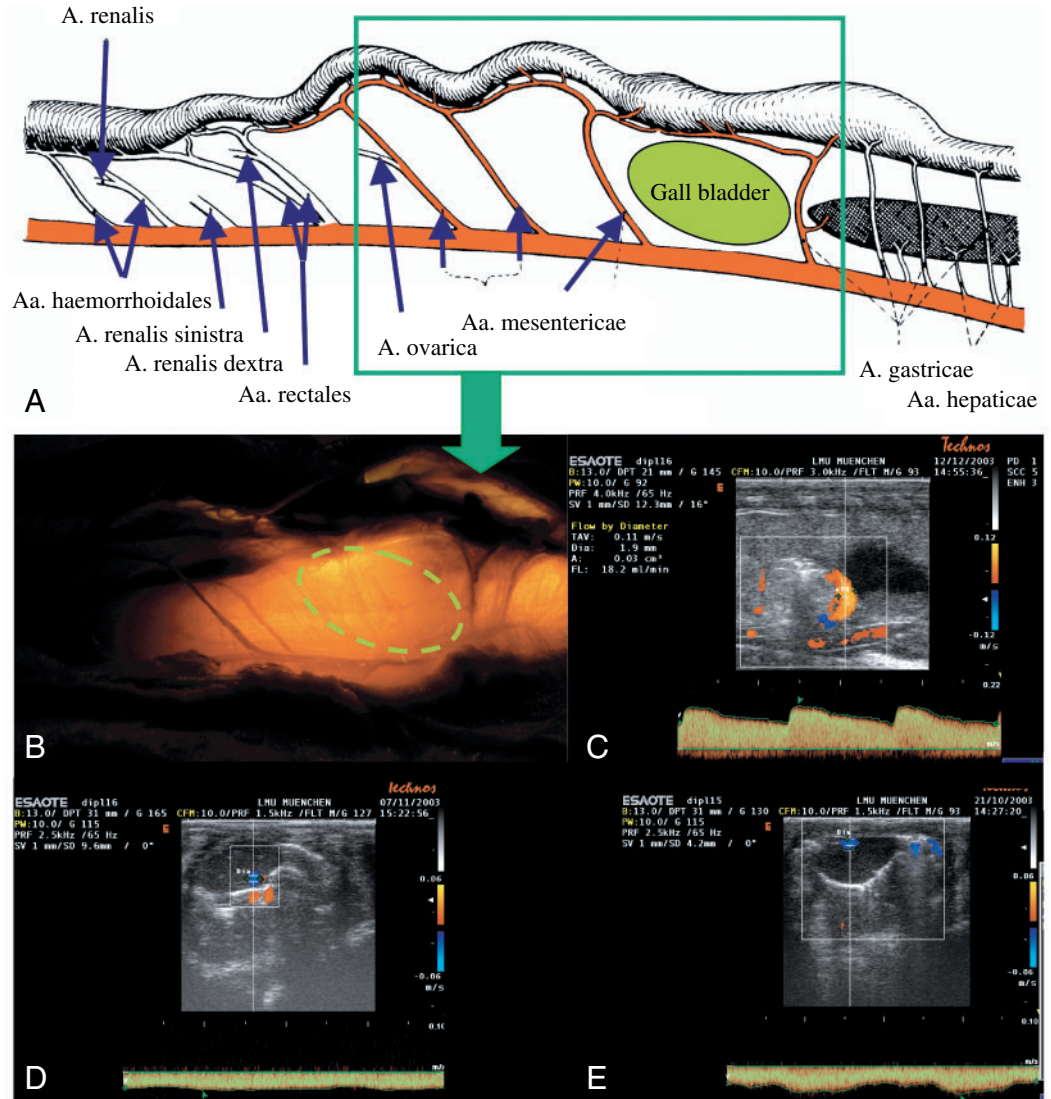
five ultrasound images per session were taken from small intestine and liver, respectively. All ultrasound images were saved in tif-format during ultrasound sessions. Ultrasound images were analyzed using the morphometry program SigmaScan v. 5.0 (Jandel Scientific). The cross section of the liver and the thickness of the mucosa of the small intestine were measured from ultrasonographs. One measurement was taken from the liver cross sections; multiple measurements were taken from the small intestinal mucosa. Doppler-ultrasound images and measured PW-spectra were saved in the Technos MP internal format and later analyzed using the morphometry options of the Esaote Technos MP. Backup files in the original format and tif-format-converted files of all images were saved on DVD for documentation. For all repeated measurements, daily means from multiple measurements were entered into statistics. None of the variables differed from normal distribution. Values given are means ± standard deviation (S.D.) of N individuals. Data were analyzed using repeated-measures analysis of covariance (RM-ANCOVA). Feeding was the inter-subject factor, day after feeding was the within-subject factor, and body mass was the covariate.

Measurements from histological slides

From histological sections, the surface magnification of the mucosal epithelium can be measured as a functional parameter of absorptive capacity of the tissue. Epithelial surface magnification was measured as the epithelial surface over a baseline defined by the inner circular muscle layer. Measurements were taken by tracing the epithelial surface with a cursor on a digitizing tablet and calculation of its total length divided by the length of the baseline, expressed as a dimensionless ratio. The amount of lipid droplets incorporated into enterocytes or hepatocytes was measured as the area occupied by lipid droplets per area mucosal epithelium. This measure does not render absolute data of the amount of lipid in enterocytes, but allowed us to calculate the relative amount of lipid in enterocytes which, for the purpose of this study, was sufficient. Similarly, the lipid loading of hepatocytes was measured as the area occupied by lipid droplets per number of
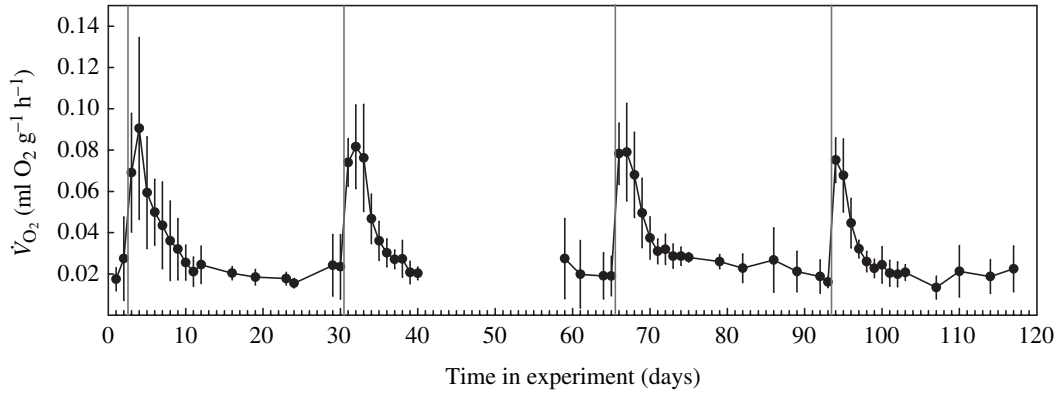
Fig. 2. Mass-specific rate of oxygen consumption $\dot{V}_{O_2}$ of ball pythons over a period of 120 days and 4 feedings. The vertical lines at days 2, 30, 65 and 93 indicate feeding. Values are means ± S.D. of 6 snakes.

hepatocytes. Five measurements were taken per section and five sections studied per individual snake. Tissue measurements were averaged by section and within each animal to avoid pseudoreplication of data. SPSS v. 11.0 was used for all statistical analyses.

Results

Vascular morphology and ultrasonography

A variable number of Arteriae (Aa) mesentericae provide the arterial blood supply to the small intestine. These arteries branch off from the Aorta descendens at an angle of about 45°. The mesenteric arteries are embedded in the connective tissue of the dorsal mesentery (Fig. 1A,B). Because of this flexible position of the arteries in the mesentery, their anatomical position varies with changing size and filling of the gastrointestinal tract, as well as with movements of the snake. The serially arranged mesenteric arteries supply subsequent regions of the small intestine, but anastomoses connect the branches of the segmental arteries before they enter the wall of the small intestine. Therefore, it is not possible to define 'supply regions' precisely for each individual artery.

Vascular ultrasonography must accommodate the variable vascular anatomy and the scanner head position needs to be adjusted to the changing positions of the vessels. Reproducible images can be obtained by placing the scanner head on the left side of the large ventral scales in the position of the gall bladder (i.e. about 1/3 SVL). The ultrasonographic image captures the posterior part of the gall bladder and the aorta in the dorsal region of the image, just below the vertebral column, as morphological landmarks. The aorta can readily be recognized by its anatomical position in the CW/PW-Doppler image (Fig. 1C) and by its pulsed pattern of arterial blood flow in caudal direction. The mesenteric arteries emerge as serial arteries from the aorta and lead to the small intestine (Fig. 1A–C). For Doppler-measurements, we consistently used the first artery that branches off from the aorta directly caudal to the gall bladder. In this artery, the blood flow has the same direction and arterial pattern as in the aorta (Fig. 1C). The Vena cava posterior is anatomically next to the aorta, but direction of flow and pattern of pulse are clearly different.

The Vena subintestinalis collects blood from the small intestine and drains it to the liver portal vein (Vena portae hepaticae). The portal vein enters the liver at its caudal tip. At this position, it carries all blood that drains from the small intestine to the liver. The liver of a snake is cigar-shaped, with an oval cross section. The portal vein extends along the entire length of the liver, where it runs along the medial (inner) side of the liver (Fig. 1D), opposite to the liver vein. Along its course, smaller vessels branch off from the portal vein and drain into the sinusoids of the liver. The liver vein (Fig. 1E) runs along the lateral (outer) side of the liver opposite to the portal vein. It collects blood from the liver and drains it to the Vena postcava before it enters the much reduced Sinus venosus of the heart. Vascular ultrasonography of the liver portal vein and the liver vein requires ultrasound cross-sections through the caudal end of the liver. The liver can easily be found in right ventro-lateral position with its caudal end just anterior to the gall bladder.

From the vascular anatomy, i.e. the serial organization of vessels and the shunts between arteries, it is evident that measurements of blood flow volume in just one mesenteric artery cannot provide quantitative data of the complete blood supply to the small intestine. Such quantitative measurements of the entire blood flow volume are, however, possible in the liver portal vein, where all blood from the small intestine enters the liver (see below).

Respirometry

The mass-specific rate of oxygen consumption of fasting snakes was 0.02 ± 0.01 ml O_2 g^{-1} h^{-1} (average of N=6 animals, each animal was measured during four successive feeding cycles). Within 24 h after feeding the oxygen consumption increased to 0.074 ± 0.006 ml O_2 g^{-1} h^{-1} and reached peak oxygen consumption 48 h after feeding at an average of 0.08 ± 0.021 ml O_2 g^{-1} h^{-1} (Fig. 2). Thereafter, oxygen consumption declined rapidly, returning to fasting values around 10 days after feeding (0.021 ± 0.004 ml O_2 g^{-1} h^{-1}). Feeding had a highly significant effect on mass-specific metabolic rate (RM-ANOVA; repeat was the inner-subject factor and feeding was between-subject factor: $F_{1,12}$=26.28, $P<0.001$).

Fig. 3. Changes of the thickness of the mucosa epithelium of ball python as measured with grey level ultrasonography over a period of 120 days and 4 feedings. The vertical lines at days 2, 30, 65 and 93 indicate feeding. Values are means ± S.D. of 6 snakes.
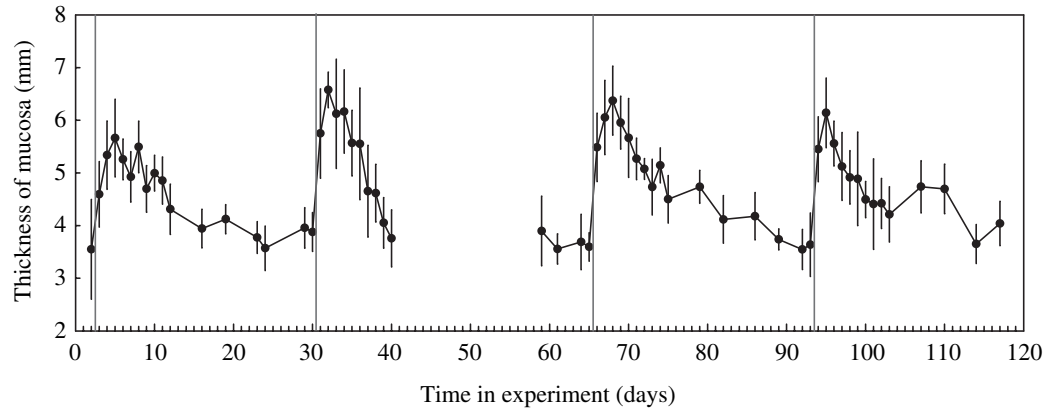
Organ size changes

Within 24 h after feeding, the thickness of the intestinal mucosa increased, as observed in ultrasonographic grey level images. In fasting snakes, the thickness of the mucosa was on average 3.73±0.27 mm (2 days before feeding; average of $N=6$ animals, each animal was measured during four successive feeding cycles). Within 3 days after feeding, the thickness of the intestinal mucosa reached peak size of 5.98±4.3 mm (Fig. 3). 3–4 days after feeding the thickness of the mucosa began to decline, reaching fasting values at about 2 weeks after feeding (3.78±0.28 mm). The described organ size changes were highly significant (RM-ANCOVA with body mass as covariate; repeat was the inner-subject factor and feeding was between-subject factor: $F_{1,12}=24.56$, $P<0.001$; body mass was not significant as a covariate).

The cross sectional diameter of the liver showed a similar pattern of increase and decrease. During the fasting periods the cross sectional diameter of the liver was 10.3±1.1 mm (2 days before feeding; average of $N=6$ animals, each animal was measured during four successive feeding cycles). 2 days after feeding the cross sectional diameter of the liver reached a peak value (12.9±1.6 mm). 2 weeks after feeding liver size had returned to prefeeding values (10.5±1.2 mm). Feeding was a highly significant effect (RM-ANCOVA with body mass as covariate, repeat was the inner-subject factor and feeding was between-subject factor; main effect feeding: $F_{1,12}=1.91$, $P=0.05$; body mass was a significant covariate: $F_{1,1}=4.63$, $P=0.035$). The factorial size increase of the liver was much smaller (on average 25%) than in the small intestine (on average 300%) and the variances were much higher. Also, the response curve was less steep and the liver took longer returning to fasting values (Fig. 4).

Patterns of blood flow

In all vessels studied, the patterns of blood flow changed in response to feeding. In the mesenteric artery, blood

flow velocity and consequently blood flow volume increased after feeding, remaining elevated for 2–3 days and then slowly returning to fasting values. The measurements of blood flow volume in the first mesenteric artery had relatively large variances. The absolute values ranged between 0.4 ml min^{-1} and 1.2 ml min^{-1} (Fig. 5A), thus values were relatively small. However, the serial arrangements of mesenteric arteries and the shunts between them indicate that one does not capture the entire blood flow volume if measurements are only taken in one artery. During fasting, blood flow volume in the first mesenteric artery was 0.69±0.11 ml min^{-1}. 1 day after feeding the blood flow volume had increased to an average of 1.0±0.12 ml min^{-1} and returned to pre-feeding values within 6 days after feeding ($N=6$ snakes, each animal being measured during four feeding cycles). Feeding as main effect and body mass as a covariate were both significant in a repeated-measures analysis (RM-ANCOVA, between-subject factor: $F_{1,12}=4.772$, $P\leqslant0.001$; covariate body mass: $F_{1,1}=13.7$, $P\leqslant0.001$).

When measured at the caudal end of the liver, the liver portal vein transports all blood that drains from the intestines to the liver. The vessel is easy to find by Doppler-ultrasonography and the signal to noise ratio is very good (Fig. 5B). During fasting, blood flow volume was on average 5.28±1.06 ml min^{-1}. Within 24 h after feeding, blood flow
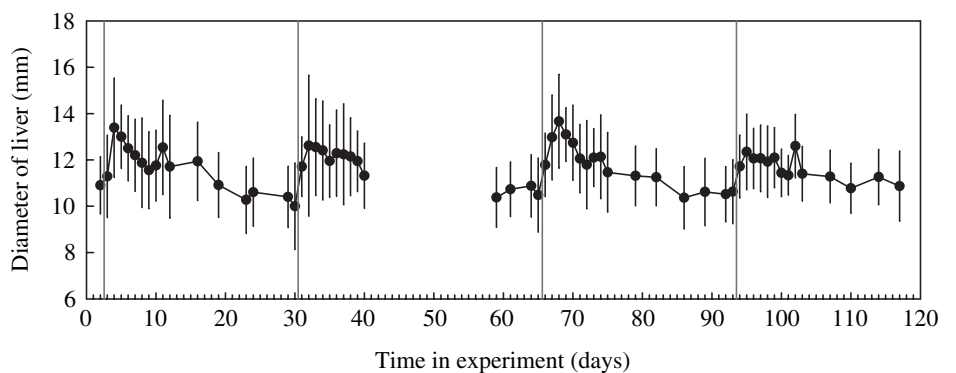

Fig. 4. Changes of the diameter of the liver of ball python ($N=6$) as measured with grey level ultrasonography over a period of 120 days and 4 feedings. The vertical lines at days 2, 30, 65 and 93 indicate feeding. Values are means ± S.D. of 6 snakes.
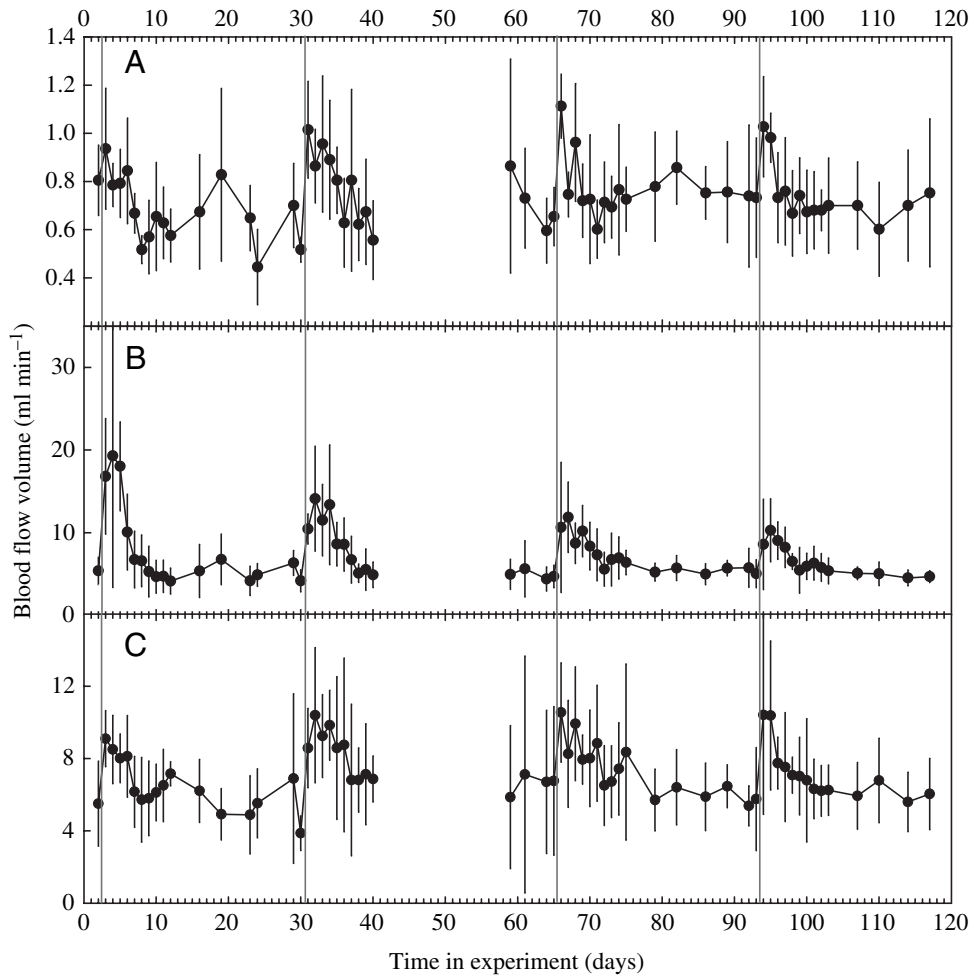
Fig. 5. Changes of blood flow volume of ball python (*N*=6) in (A) the mesenteric artery, (B) the liver portal vein and (C) the liver vein. Values are means ± S.D. of 6 snakes.

of the between-subject factor 'feeding' and the covariate 'body mass' on blood flow volume in the liver vein were both highly significant (RM-ANCOVA repeat was the inner-subject factor and feeding was between-subject factor; between-subject factor: $F_{1,12}$=5.72, $P \leqslant 0.001$; covariate body mass: $F_{1,1}$=107.7; $P \leqslant 0.001$). A continuous blood flow as typical for veins was observed.

The liver portal vein showed the best Doppler-signal of blood flow volume. This is based on its easy accessibility to Doppler-ultrasound imaging and to the fact that it carries all blood passing from the small intestine to the liver. Therefore in the following analyses, blood flow volume in the liver portal vein was used for correlations to the observed changes of organ size of small intestine and liver. To account for possible body size effects, all values were transformed into relative values with the fasting value (i.e. 2 days before feeding) being 100%. A nonlinear regression of mucosal thickness as dependent variable of blood flow volume resulted in a highly significant correlation (Fig. 6; ANOVA, F=68.29, $P \leqslant 0.001$, r^2=0.54). The correlation explained over 50% of overall variation in mucosal thickness. A nonlinear regression of liver size on blood flow volume also showed a tight relationship between both variables and explained more than 50% of the overall variation in liver size (Fig. 7; ANOVA, F=61.24, $P \leqslant 0.001$, r^2=0.51). Interestingly, the relationship between blood flow volume and organ size followed an exponential function for small intestine and liver indicating limitations, i.e. increase in blood flow volume resulted in only a limited range of values in an increase of mucosal thickness or liver size.

Histological changes and morphometry

When fasting, the mucosal epithelium was pseudostratified and the enterocytes contained no lipid droplets, as described previously for other snake species (Starck and Beese, 2001, 2002). Within 24 h after feeding the enterocytes were loaded with lipid droplets and the epithelium changed into a single layered configuration (Fig. 8A,B). Also, the brush border of enterocytes was much more prominent after feeding and the connective tissue core of the villi showed enlarged capillaries and lymphatic vessels. No differences were found in the tissues
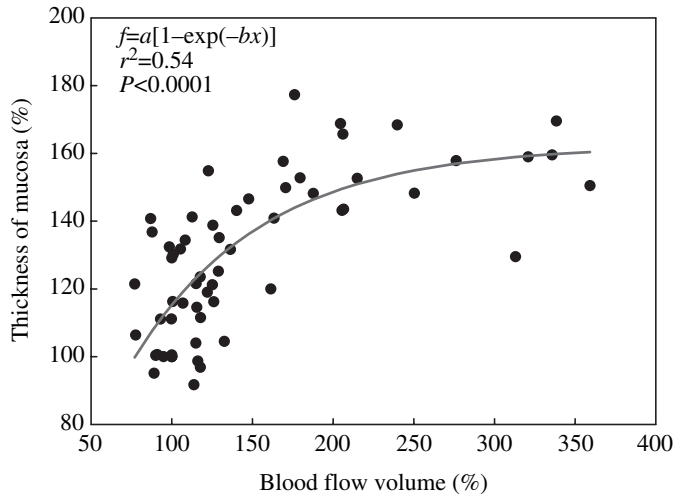
volume reached a peak at an average of 14.01±4.56 ml min⁻¹. Within 1 week after feeding, the value declined again to fasting values (5.87±1.36 ml min⁻¹). Feeding as main effect and body mass as the covariate were both highly significant on blood flow volume in the liver portal vein (RM-ANCOVA, repeat was the inner-subject factor and feeding was between-subject factor; between-subject factor: $F_{1,12}$=12.56, $P \leqslant 0.001$; covariate body mass: $F_{1,1}$=36.2, $P \leqslant 0.001$). Blood flow in the liver portal vein does not show a pulse; flow is continuous.

Not unexpectedly, the liver vein showed a very similar pattern to that described for the liver portal vein (Fig. 5C). However, the absolute values of measurement were smaller than in the portal vein because at the measurement position only about 50% of the blood flowing from the liver to the heart was captured. The blood flow volume in fasting snakes was on average 5.5±2.19 ml min⁻¹. Within 24 h after feeding, it increased to 9.29±1.81 ml min⁻¹ (*N*=6 snakes, each animal being measured four times). Within 2 weeks after feeding, it returned to fasting values; however, our measurements showed relatively high variances that made it difficult to determine precisely when values had returned to fasting values. Effects

Fig. 6. Nonlinear regression of thickness of mucosal epithelium and blood flow volume.

Fig. 7. Nonlinear regression of thickness of liver cross sectional diameter and blood flow volume.

of the snakes that had been digesting their prey for either 24 or 48 h, respectively.

Associated with lipid loading of enterocytes the surface magnification increased significantly from 13.82±3.0 to 62.9±2.6, i.e. by a factor 4.5 (*t*-test, *T*=19.62, *P*<0.001). In digesting snakes, lipid droplets occupied on average 35% of the epithelial area (Fig. 8B). When surface magnification was regressed as on area of lipid droplets, a highly significant linear correlation was detected, i.e. surface magnification increased significantly with increasing lipid loading of enterocytes. The relationship explained approximately 60% (regression: slope=0.09, intercept=8.45, *r*²=0.62; ANOVA, *F*=33.98, *P*<0.001) of the overall variation in the small intestine's surface magnification.

Similar changes were observed in the liver. The hepatocytes of fasting snakes contained no lipid droplets (Fig. 8C). Within 24 (48) h after feeding the hepatocytes were filled with lipid droplets. The area per section occupied by lipid droplets increased from a fasting value of 2.8±1% to 17±1.3% after feeding (Fig. 8D). It was not possible to calculate a correlation of liver cross-sectional diameter on area of lipid droplets because these measurements were not taken from the same individuals. However, the results are so clear that a relationship between loading of hepatocytes with lipid droplets and liver size can safely be postulated; i.e. liver size increases as hepatocytes become loaded with lipid droplets after feeding.

Discussion

The vascular anatomy of ball python resembles that of *Boa* sp. (Hafferl, 1933). Understanding the vascular anatomy is not only important for a correct interpretation of ultrasonographs, but also particularly important when determining the Doppler-positions for blood flow volume measurement. Clearly, the shunts between the mesenteric arteries supplying the small intestine prohibit quantitative measurements on the supply side of the vascular system; however, measurements in the arteries
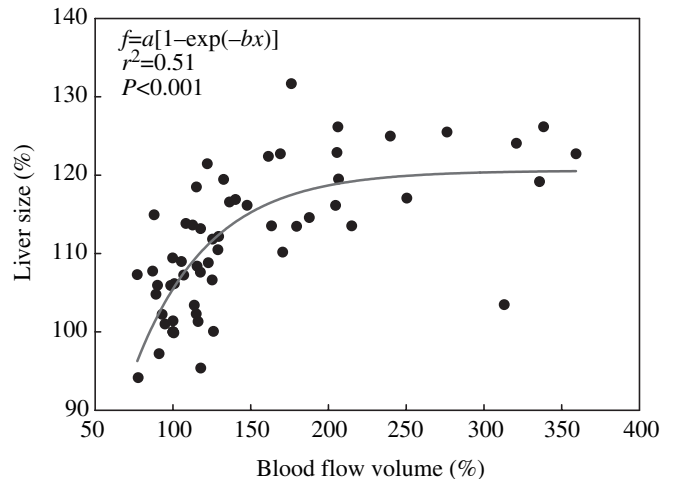
reveal relative changes in blood flow volume. Because what goes in must come out, the blood flow volume to the gut can also be measured in the caudal part of the liver portal vein. At this position all blood that had been delivered to the gut through the mesenteric arteries is (re)collected and thus offers a better position for quantitative measures of blood flow volume to/from the gastrointestinal tract.

In ectotherm sauropsids, postprandial upregulation of metabolic rate is affected by a variety of factors, e.g. temperature, meal size, composition of diet and feeding frequency (Secor and Diamond, 1997; Wang et al., 2003; Andrade et al., 2005; McCue et al., 2005). A 4-factorial increase of rate of oxygen consumption as reported here for snakes feeding a prey of 25% of their body mass, and kept at temperatures of 25–30°C, is well within the range of previously reported values (Overgaard et al., 1999, 2002; Starck et al., 2004; Andrade et al., 2005). Thus, the ball pythons in this experiment performed a regular and undisturbed postprandial upregulation of metabolic rate. Also, the organ size changes observed here showed the same pattern and same values of up- and downregulation as reported earlier for another python species (Starck and Beese, 2001, 2002; Starck et al., 2004). The histological samples necessarily had to be taken from a different group of individual snakes. The configuration changes observed in the tissue and the loading of cells with lipid droplets followed the pattern described earlier for Burmese pythons (Starck and Beese, 2001), garter snakes (Starck and Beese, 2002) and other ectotherm sauropsids (Starck, 2003, 2005). Thus, it is safe to say that the ball pythons in the experiment performed a postprandial response that did not differ from that seen in other snake species.

Changes in blood flow volume were clearly correlated with the postprandial upregulation of organ size in ball pythons. The correlations explain about 50% of the variation in organ size changes as a correlated response to increased blood flow volume. Thus, the nonlinear regressions in Figs 6 and 7 support the hypothesis that the postprandial increase of mucosal

Fig. 8. Histology of the mucosal epithelium and liver of ball python. (A) The mucosal epithelium of fasting snakes is a pseudostratified epithelium in which nuclei of enterocytes are arranged in several layers. (B) 24 h after feeding the enterocytes are loaded with lipid droplets and the epithelium has changed into a single layered epithelium. Note the prominent brush border of the enterocytes. (C) Liver parenchyma of fasting snakes. Hepatocytes are relatively small, and only a few vesicles can be found within them. (D) Liver parenchyme 24 h after feeding. The hepatocytes are loaded with lipid droplets. Scale bars, 50 µm.
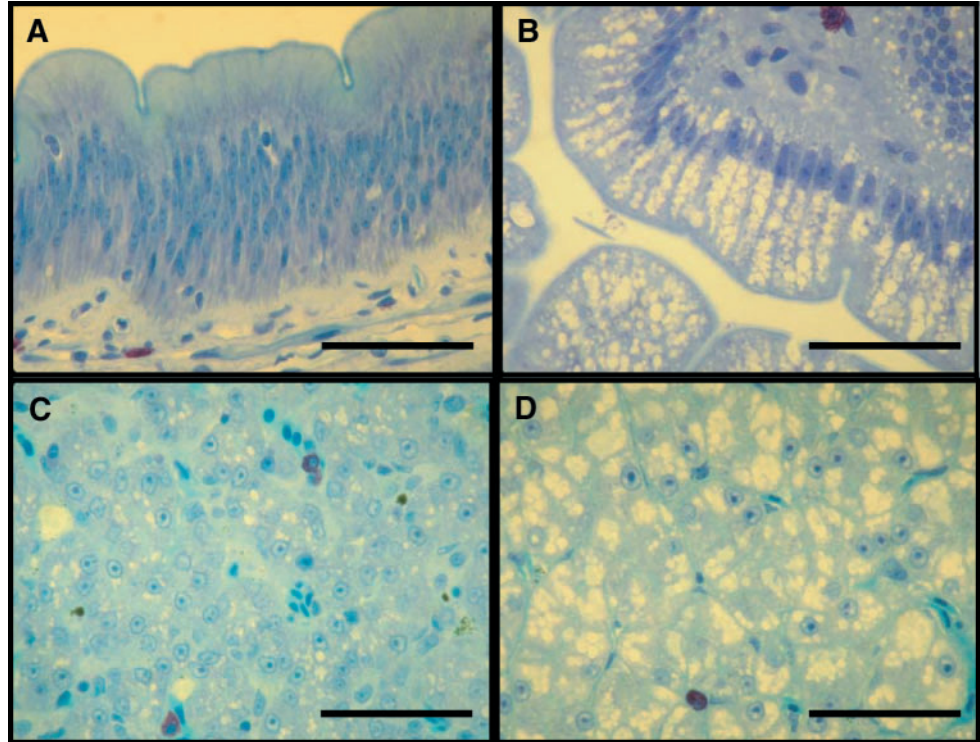
thickness and liver size is partially related to increasing blood flow volume to these organs. Although the correlations support the hydraulic pump hypothesis, the relationship is not linear and not straight. Obviously, a change in blood flow volume results in increasing mucosal surface only in a restricted range, reaching an upper limit at about 150%–200% blood flow volume of fasting value. Above this value, a further increase in blood flow volume does not result in continued increase of mucosal thickness. Identical observations have been made for the liver. A second factor contributing to organ size increase is loading of cells with lipid droplets. Enterocytes and hepatocytes are loaded with lipid droplets. Organ size/cell size is clearly correlated with the amount of lipid droplets in the cells, explaining approximately another 50% of overall variation in organ size.

In summary, the data presented here support the hydraulic pump hypothesis, i.e. by pumping more blood into the vessels of the small intestine the villi elongate and provide a larger absorptive surface to the digesta. In addition, loading of the enterocytes with lipid droplets also contributes considerably to an increase of the mucosal surface magnification. Of course, data on blood flow volume and increasing enterocytes size were necessarily obtained from different animals and therefore cannot be combined in one analysis. However, both data sets are clear enough to safely conclude that increasing blood flow the organ and loading of cells with lipid droplets both contribute to the organ size increase of small intestine and liver after feeding. The exact partitioning of the contribution of both processes ought to be determined. Also, increased flow of lymphatic fluid into the villi might contribute to the overall enlargement of the small intestine. The results of this study match the previously published observation that cell proliferation is not involved in the upregulation of small intestine size or liver (Starck and Beese, 2001, 2002). Recently published analyses showed that the increase of small intestine size is an energetically cheap process (Overgaard et al., 2002; Secor, 2003; Starck et al., 2004). Downregulation of organ size is obviously associated with declining blood flow volume and transport of lipid droplets to the adipose tissue depots. On that basis, one might even speculate that the up- and downregulation of organ size are just byproducts of digestion, with blood being pumped to the gut to enhance transport of absorbed nutrients from the gut to the liver, while loading of enterocytes with lipid droplets occurs during lipid absorption. For the liver, the processes are supposedly very similar and may also be understood as byproducts of general activation of the digestive system. The delayed response in size change of the liver as compared to the small intestine supports this interpretation.

References

Andrade, D. V., Cruz-Neto, A. P., Abe, A. S. and Wang, T. (2005). Specific dynamic action in ectothermic vertebrates: a general review on the

determinants of post-prandial metabolic response in fishes, amphibians, and reptiles. In *Physiological and Ecological Adaptations to Feeding in Vertebrates* (ed. J. M. Starck and T. Wang), pp. 305-324. Enfield, NH, USA: Science Publishers.

Bedford, G. S. and Christian, K. A. (2001). Metabolic response to feeding and fasting in the water python *(Liasis fiscus)*. *Austral. J. Zool.* **49**, 379-387.

Hafferl, A. (1933). Das Arteriensystem. In *Handbuch der vergleichenden Anatomie der Wirbeltiere*, Vol. 6 (ed. L. Bolk, E. Göppert, E. Kallius and W. Lubosch), pp. 563-684. Berlin: Urban and Schwarzenberg.

McCue, M. D., Bennett, A. F. and Hicks, J. W. (2005). The effect of meal composition on specific dynamic action in Burmese pythons (*Python molurus*). *Physiol. Biochem. Zool.* In press.

Overgaard, J., Andersen, J. B. and Wang, T. (2002). The effects of fasting duration on the metabolic response to feeding in *Python molurus*: an evaluation of the energetic costs associated with gastrointestinal growth and upregulation. *Physiol. Biochem. Zool.* **75**, 360-368.

Overgaard, J., Busk, M., Hicks, J. W., Jensen, F. B. and Wang, T. (1999). Respiratory consequences of feeding in the snake *Python molurus. Comp. Biochem. Physiol.* **124A**, 359-365.

Secor, S. M. (2003). Gastric function and its contribution to the postprandial metabolic response of the Burmese pythons *Python molurus. J. Exp. Biol.* **206**, 1621-1630.

Secor, S. M. and Diamond, J. (1995). Adaptive responses to feeding in Burmese pythons: pay before pumping. *J. Exp. Biol.* **198**, 1313-1325.

Secor, S. M. and Diamond, J. (1997). Determinants of postfeeding metabolic response in Burmese python, *Python molurus. Physiol. Zool.* **70**, 202-212.

Secor, S. M. and Diamond, J. (1998). A vertebrate model of extreme physiological regulation. *Nature* **395**, 659-662.

Secor, S. M. and Diamond, J. (2000). Evolution of regulatory response to feeding in snakes. *Physiol. Biochem. Zool.* **73**, 123-141.

Secor, S. M., Stein, E. D. and Diamond, J. (1994). Rapid upregulation of snake intestine in response to feeding: a new model of intestinal adaptation. *Am. J. Physiol.* **266**, G695-G705.

Starck, J. M. (1999). Structural flexibility of the gastro-intestinal tract of vertebrates. Implications for evolutionary morphology. *Zool. Anz.* **238**, 87-101.

Starck, J. M. (2003). Shaping up: how vertebrates adjusts their morphology to changing environmental conditions. *Animal Biol.* **53**, 245-257.

Starck, J. M. (2005). Structural flexibility of the digestive system of tetrapods – Patterns and processes at the cellular and tissue level. In *Physiological and Ecological Adaptations to Feeding in Vertebrates* (ed. J. M. Starck and T. Wang), pp. 175-200. Enfield, NH, USA: Science Publishers.

Starck, J. M. and Beese, K. (2001). Structural flexibility of the intestine of Burmese python in response to feeding. *J. Exp. Biol.* **204**, 325-335.

Starck, J. M. and Beese, K. (2002). Structural flexibility of the small intestine and liver of garter snakes in response to feeding and fasting. *J. Exp. Biol.* **205**, 1377-1388.

Starck, J. M. and Burann, A. K. (1998). Noninvasive imaging of the intestinal tract of snakes: A comparison of normal anatomy, radiography, magnetic resonance imaging, and ultrasonography. *Zoology* **101**, 210-223.

Starck, J. M., Dietz, M. and Piersma, T. (2001). Ultrasound scanning. In *Body Composition Analysis: A Handbook of Non-Destructive Methods,* Chapter 7 (ed. J. R. Speakman), pp. 188-210. Cambridge: Cambridge University Press.

Starck, J. M., Moser, P., Werner, R. and Linke, P. (2004). Pythons metabolize prey to fuel the response to feeding. *Proc. R. Soc. Lond. B* **271**, 903-908.

Thompson, G. G. and Withers, P. C. (1999). Effect of sloughing and digestion on metabolic rate in the Australian carpet python, *Morelia spilota impricata. Austral. J. Zool.* **47**, 605-610.

Wang, T., Andersen, J. B. and Hicks, J. W. (2005). Effects of digestion on the respiratory and cardiovascular physiology of amphibians and reptiles. In *Physiological and Ecological Adaptations to Feeding in Vertebrates* (ed. J. M. Starck and T. Wang), pp. 279-303. Enfield, NH, USA: Science Publishers.

Wang, T., Zaar, M., Arvedsen, S., Vedel-Smith, C. and Overgaard, J. (2003). Effects of temperature on the metabolic response to feeding in *Python molurus. Comp. Biochem. Physiol.* **133A**, 519-527.